FISEVIER

Contents lists available at ScienceDirect

Developments in the Built Environment

journal homepage: www.sciencedirect.com/journal/developments-in-the-built-environment





Synergistic modification of bamboo aggregates by sodium alginate-CaCl₂: optimization and performance evaluation of sustainable lightweight concrete

Xiang Chen ^{a,b}, Hongzhou Zhu ^{b,c}, Xinqiang Zhang ^{d,*}, Dan Yang ^b, Zhenzhen Wang ^a, Jian Zhang ^e, Jian Zhang ^{f,**}

- ^a School of Civil Engineering, Chongqing Three Gorges University, Chongqing, China
- ^b School of Civil Engineering, Chongqing Jiaotong University, Chongqing, China
- ^c National & Local Joint Engineering Research Center of Transportation and Civil Engineering Materials, Chongqing Jiaotong University, Chongqing, China
- ^d Department of Civil and Environmental Engineering, The Hong Kong Polytechnic University, Hong Kong, China
- ^e Lanzhou Mineral Exploration Institute of Gansu Nonferrous Metal Geological Exploration Bureau, Lanzhou, China
- f College of Civil and Transportation Engineering, Shenzhen University, Shenzhen, China

ARTICLE INFO

Keywords: Bamboo aggregate concrete Sodium alginate Compressive strength Bamboo aggregate mass index (BAMI) Sustainable construction materials

ABSTRACT

In the context of global climate change, the demand for green building materials has grown increasingly urgent. This study has made significant advancements in sustainable construction materials by developing all-bamboo aggregate concrete (BAC) enhanced with a sodium alginate- $CaCl_2$ synergy through an environmentally friendly process. Using response surface methodology optimization, the 28-day compressive strength was increased to 8.10 MPa. Scanning electron microscope (SEM) analysis indicates that the alginate gel forms a cross-linked network within bamboo micro-cracks, substantially improving interfacial bonding. A novel bamboo aggregate mass index (BAMI) has been introduced to quantify particle shape, allowing precise control over aggregate quality, thus offering a new solution for lightweight pavement materials. While fly ash reduces short-term strength, its low alkalinity and secondary hydration effects positively influence long-term durability. This research provides a scientific basis for utilizing BAC in pedestrian pavements and advancing sustainable construction materials.

1. Introduction

In recent years, the escalating awareness of environmental protection and the pursuit of sustainable development have thrust the construction industry into an urgent quest to reduce carbon emissions and resource consumption (Li et al., 2025). This imperative has ignited a surge of interest in sustainable construction materials, with bamboo-based materials emerging as a highly promising frontier. Bamboo, with its extensive global distribution and rapid growth rate, stands out as a sustainable green material with potential in the construction sector (Mohan et al., 2022; van der Lugt et al., 2006; Yu et al., 2011). Bamboo fiber-reinforced composites have demonstrated significant potential in improving the structural integrity of reinforced

concrete beams, as explored in various innovative applications (Chin et al., 2020). Comprehensive assessments of the environmental impacts of bamboo-based construction materials across diverse global production scenarios have underscored their sustainability (Escamilla and Habert, 2014). Moreover, critical properties such as the water vapor diffusion resistance factor of Moso bamboo have been investigated to better understand its performance in different environmental conditions (Huang et al., 2017). Collectively, these studies highlight bamboo's suitability as a sustainable building material. The development of bamboo aggregate concrete has gained traction as an approach to reduce reliance on traditional gravel and mitigate the environmental impact of natural stone extraction. Experimental studies have demonstrated the feasibility of partially replacing coarse aggregate with bamboo in

This article is part of a special issue entitled: Upcycling of Waste published in Developments in the Built Environment.

E-mail address: zhangxq0112@126.com (X. Zhang).

https://doi.org/10.1016/j.dibe.2025.100670

^{*} Corresponding author.

^{**} Corresponding author.

concrete (Manimaran et al., 2017; Mudjanarko et al., 2020; Sari et al., 2020; Tahara et al., 2021), further bolstering the evidence for bamboo aggregate's potential in construction.

However, using bamboo aggregates in concrete faces numerous challenges due to their biomass traits. Compared with traditional aggregates, bamboo aggregates have problems such as volume instability, alkali degradation, and the impact of sugars on concrete setting and hardening (Li et al., 2022; Wang et al., 2022, 2024a; Yuan et al., 2022). For example, the volume of bamboo aggregates can change significantly with humidity, which lead to cracks in concrete. The alkali in concrete can react with the components in bamboo, causing degradation of the aggregates. The sugars in bamboo can also affect the setting and hardening process of concrete, reducing its strength. One of the effective solutions is to conduct appropriate modification treatments on bamboo aggregates (Idris et al., 2021; Wang et al., 2024b; Zhou et al., 2024). However, there are no modification methods specifically for bamboo aggregates in all-bamboo aggregate concrete (BAC).

This study aims to systematically compare various modification methods of bamboo aggregates to identify the most effective approach for enhancing the compressive strength of BAC. Using response surface methodology, the parameters of the chosen modification method will be optimized to achieve optimal BAC performance. The physical and mechanical properties of modified BAC will be comprehensively analyzed, with a focus on factors such as bamboo aggregate grading and fly ash content. Scanning electron microscope (SEM) analysis will be employed to gain an in-depth understanding of the modification mechanisms at play. The results of this study will provide a scientific basis for the application of BAC in pedestrian walkway pavements and offer new perspectives on promoting the use of sustainable building materials.

2. Experimental part

2.1. Experimental materials

P.O 42.5 ordinary Portland cement, produced locally in Chongqing, was used as the binder. Moso bamboo from the Tanghe Ancient Town Forest Farm in Jiangjin, Chongqing, with a $3\sim5$ -year growth period, about 10 cm in diameter and 10-15 mm in wall thickness, was used to produce bamboo aggregates. After crushing, their particle size was mostly 5-15 mm, as shown in Fig. 1, and they were then modified and dried to enhance compatibility with other components and improve concrete performance. Tested in accordance with the "Quality and

Inspection Methods Standard for Sand and Stone for General Concrete" (JGJ52-2006), the fineness modulus of the employed river sand is 3.0; its grading curve is presented in Fig. 2, and this river sand is classified as medium sand and is utilized to fill the voids in the concrete, thereby enhancing the workability and strength of the concrete. A polycarboxylate-based water reducer was used to reduce water content, optimize the water-cement ratio (W/C), maintain or enhance workability, and improve mechanical properties, whose basic properties are listed in Table 1. Calcium chloride was employed as the accelerator to accelerate the setting and hardening of concrete, especially useful in applications requiring rapid early-strength development. Welan gum was added to enhance the cohesiveness of the concrete mixture, prevent mortar weeping, and improve workability, with its optimal dosage determined by specific experimental methods (Chen et al., 2024). Class II fly ash from Henan, whose chemical composition and basic performance parameters are shown in Tables 2 and 3, was used in this study.

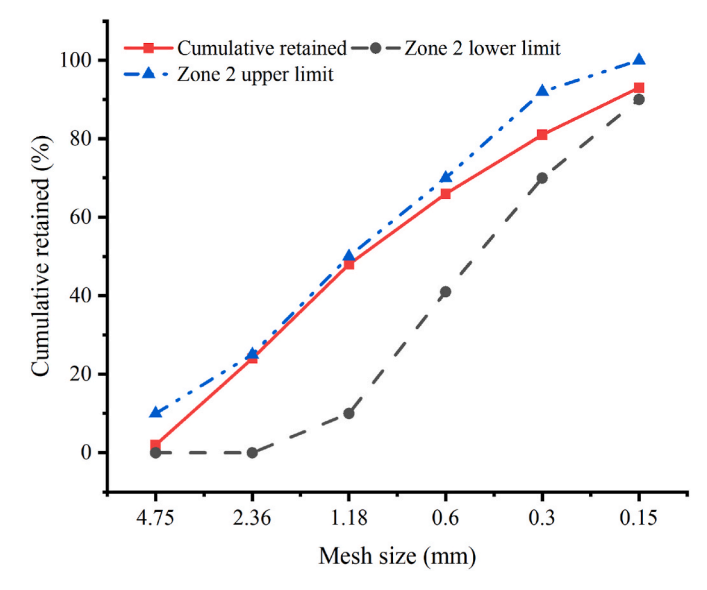


Fig. 2. Sand grading curve.



Fig. 1. Preparation process of raw bamboo aggregates.

Table 1Performance index of polycarboxylic acid superplasticizer.

| Type | pН | Solid content (%) | Total alkali content (%) | Density (g/cm ³) | Water reduction rate (%) |
|--|-----|-------------------------|-----------------------------------|---------------------------------|--------------------------------|
| Polycarboxylic acid superplasticizer | 6.1 | 39.2 | 1.05 | 1.06 | 30 |

Table 2
Chemical composition of fly ash.

| Chemical composition | SiO_2 | Al_2O_3 | Fe_2O_3 | CaO | MgO | SO_3 |
|----------------------|---------|-----------|-----------|-----|------|--------|
| Content (%) | 53.24 | 27.87 | 4.11 | 4.7 | 1.35 | 1.2 |

Table 3Basic performance parameters of fly ash.

| Fineness (%) | | requirement | Apparent density (g/ | Moisture content | | Activity index (%) | |
|-----------------|------|-------------------|-------------------------|---------------------|-----|--------------------|--|
| | | cm ³) | (%) | 7d | 28d | | |
| 17.5 | 3.54 | 103 | 2.4 | 0.1 | | | |
| | | | | | 76 | | |

2.2. Modification of bamboo aggregate

To address issues such as the high water absorption of bamboo aggregates, the negative impact of their sugar on setting and hardening, and to strengthen the bond with mortar, seven modifying agents were selected. First, establish the general pre-treatment steps for bamboo aggregates: Heat the bamboo aggregates at 103 °C for 1 h, then cool them to 70 °C and air-dry to a constant weight. Subsequent treatments with different modifying agents are carried out with differential operations based on this. The nano-penetrating agent, suitable for cement concrete with waterproof, permeation-resistant, UV-resistant, acid-andalkali-resistant, and chlorine-ion-resistant properties, is prepared by mixing with water at a 1:3 ratio. The pre-treated bamboo aggregates are immersed in it for 3 h and then air-dried naturally for 24 h. The silane impregnating agent, which is waterproof and alkali-resistant, is used undiluted, and the treatment process for bamboo aggregates is the same as that of the nano-penetrating agent. The silane coupling agent KH560, catalyzed by ethylenediamine (10 % of its quantity), has a soaking solution composed of ethanol, water, and KH560 at a ratio of 7.2:0.8:2. After the general pre-treatment, the soaking solution is heated to 60 $^{\circ}\text{C}\textsc{,}$ and the bamboo aggregates are soaked in this solution for 3 h, then heated at 103 °C for 1 h and dried at 70 °C until air-dry. It reacts with the surface hydroxyl groups of bamboo aggregates and participates in cement hydration (Chen et al., 2022). The sodium silicate solution (1 % wt.%), rich in Si-OH groups, is used in the following way. After the initial pre-treatment, the bamboo aggregates are soaked in a 60 °C solution for 3 h, then heated at 120 °C for 1 h and dried at 70 °C until air-dry. It participates in cement hydration and reacts with the surface hydroxyls of bamboo aggregates to enhance the bond (Lima et al., 2008; Liu et al., 2012). Sodium alginate, an eco-friendly extract from brown seaweed, is utilized for the modification of bamboo aggregates. The modification involves using a solution containing 0.25 % sodium alginate and 1.0 % calcium chloride. When sodium alginate is dissolved in an aqueous solution, it forms a viscous gel matrix via Ca²⁺ cross-linking, which is of great significance for the modification of bamboo aggregates. First, the bamboo aggregates are soaked in a 60 °C sodium alginate solution for 1 h and then removed. Subsequently, calcium chloride is added to the sodium alginate solution to prepare a new mixed solution, with continuous stirring. Then, the bamboo aggregates are transferred to

this newly formed mixed solution at 60 °C and soaked for 2 h. Finally, the bamboo aggregates are dried at 70 °C. During this process, sodium alginate forms a gel film with Ca²⁺, thereby enhancing the bonding performance (Blandino et al., 1999; Zactiti and Kieckbusch, 2009). The hydrophobic aluminate ester, when melted above 85 °C, can cover the bamboo aggregates. It is heated to 90 °C (turned into a liquid state) and sprayed on the air-dried bamboo aggregates (after pre-treatment), and then air-dried for 5 min to reduce water absorption and the impact of sugar, thus improving durability (Ban et al., 2020). The polyacrylate emulsion, which relies on prolonged penetration to allow sufficient diffusion of polymer chains into the internal pores of bamboo aggregates, is applied as follows: After pre-treatment, the bamboo aggregates are soaked in a 10 % emulsion for 24 h (significantly longer than the soaking times of other methods that utilize elevated temperatures or chemical reactions to accelerate the modification process) and then air-dried naturally. This extended duration ensures the formation of dense internal blockages and surface films, effectively enhancing strength and durability (Birniwa et al., 2023; Kang et al., 2014; Liu et al.,

2.3. Preparation and curing of BAC specimens

As a lightweight aggregate, bamboo aggregate has a high water absorption rate, which requires careful consideration of the water-cement ratio and the addition of water-reducing agents. During the preliminary experiments of preparing BAC mixtures, it was found that the cement mortar did not easily coat the bamboo aggregate, leading to severe weeping of the mixture. Through literature review and experimental trials, the use of Welan gum was found to effectively resolve this issue. After several adjustments to the mix ratio, the experimental mix ratio was determined, as shown in Table 4.

The mass ratios of bamboo aggregates of 5-10 mm and 10-15 mm were set at 4:6. The mass of bamboo aggregate in the table refers to the oven-dry mass. In the initial exploratory experiments, it was found that BAC made with some of the modified bamboo aggregates had a slow setting and hardening process, and the 28-day compressive strength was below 2 MPa. In this study, 5 % accelerator was first added to preliminarily analyze and compare the effects of promoting the setting and hardening of BAC. The mixing process of BAC is shown in Fig. 3. The fresh concrete was poured into 100-mm cubic molds in two layers and compacted using a flat-plate vibrator with a driving unit rotation speed of 3000 r/min and an amplitude of 1 mm pressing on the top of the mold. The use of a flat plate vibrator with specific specifications ensured proper compaction of the concrete mixture, which is crucial for the formation of a dense structure and the development of strength. After 24 h, the specimens were demolded and labeled. The demolded specimens were then subjected to standard curing conditions, which included curing in a humid environment with a temperature of 20 \pm 2 $^{\circ}$ C and a relative humidity of 95 % \pm 5 % for the specified curing periods. When preparing ordinary concrete (OC), maintain the packing volume of crushed stone equal to the packing volume of bamboo aggregate, the volume proportion of bamboo aggregate in the concrete is 42 %, do not use accelerators, and keep the other parameters the same as the BAC mix proportions.

2.4. SEM sample preparation

Bamboo slices measuring 5 mm \times 5 mm \times 3 mm (length \times width \times

Table 4BAC experimental mix proportion.

| Cement (kg/m³) | Water (kg/m³) | Bamboo aggregates (kg/m³) | Sand (kg/ m³) | W/ C | Welan gum (%) | Water reducer (%) |
|----------------|------------------|---------------------------------|---------------------|---------|---------------------|-------------------------|
| 410.4 | 258.6 | 275 | 508.9 | 0.63 | 0.5 | 0.1 |

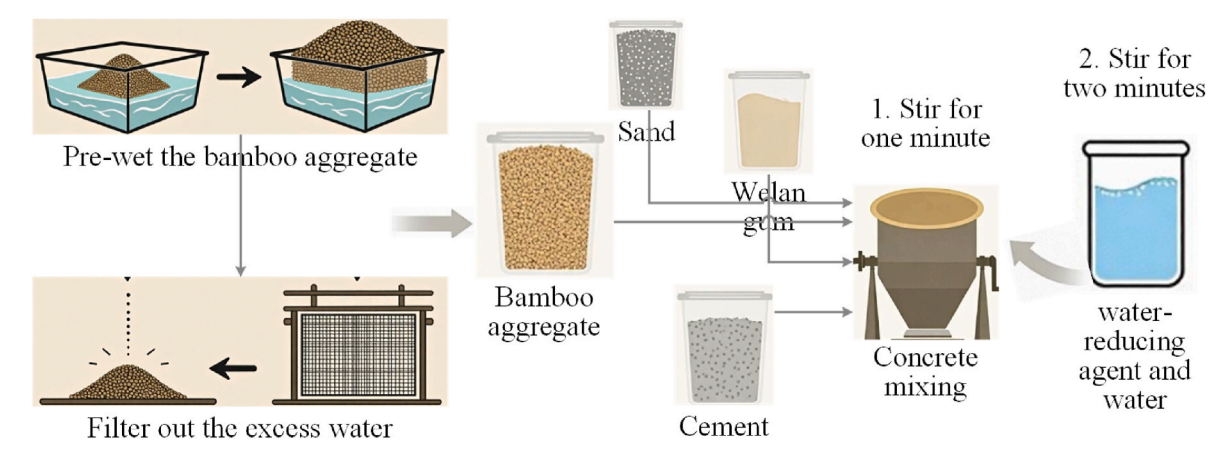


Fig. 3. The mixing process of BAC.

thickness) was prepared for SEM observation. The slices were modified according to the bamboo aggregate modification method. After modification, the samples were vacuum-gold-coated to improve the surface conductivity. The equipment used for SEM observation was the FEINOVA NANO 230 from the USA, with Au as the coating target material, a resolution of 1.0 nm (at 15 kV), magnification ranges from 200 to 200000, and an acceleration voltage of 1–30 kV. The sample preparation process was carefully controlled to ensure that the observed microstructure accurately represented the modified bamboo aggregate.

2.5. BAC specimen physical and mechanical properties test

The compressive strength of $100~\text{mm} \times 100~\text{mm} \times 100~\text{mm}$ cubic specimens was tested according to the methods specified in the "Standard for Test Methods of Physical and Mechanical Properties of Ordinary Concrete" (GB/T50081-2019). The compressive strength is determined by three test values, accurate to 0.1 MPa. If the difference between the maximum or minimum value and the median value of the three measurements exceeds 15 % of the median value, the compressive strength of that group of specimens will be taken as the median value. If the difference between both the maximum and minimum values and the median value exceeds 15 % of the median value, the results of that group are invalid. The compressive strength is calculated using Equation (1):

$$f_{cc} = \frac{F}{A} \times 0.95 \tag{1}$$

In the equation, F is the failure load of the specimen (N), A is the bearing area of the specimen (mm²), and fcc is the cubic compressive strength (MPa).

According to the "Technical Standard for Application of Lightweight Aggregate Concrete" (JGJ/T 12–2019), the overall oven-drying method is used. The specimens are placed in an oven at $105\sim110$ °C to dry to a constant weight and the volume of the specimens is measured. The dry apparent density of the concrete is calculated using Equation (2):

$$\rho = \frac{m}{V} \times 10^3 \tag{2}$$

In the equation, m represents the mass of the specimen after drying (g), V represents the volume of the specimen after drying (cm³), and ρ represents the dry apparent density of the specimen (kg/m³).

The water absorption test involves drying the specimens to a constant weight, then immersing them in water at a temperature of 20 \pm 5 °C for 48 h. After soaking, the specimens are removed, wiped dry with a cloth, and weighed. The average value of three specimens is taken. The water absorption of the concrete is calculated using Equation (3):

$$\omega_{sat} = \frac{m_n - m_0}{m_0} \times 100\% \tag{3}$$

In the equation, m_0 represents the average mass of the specimens dried to a constant weight (g), m_n represents the average mass of the specimens after 48 h of water immersion (g), and ω_{sat} represents the water absorption rate after 48 h of immersion (%).

3. Experimental results and analysis

3.1. The effect of different modification methods on BAC strength

Fig. 4(a) and (b) shows the compressive strength of BAC with different modifications at curing ages of 14-day and 28-day. For the unmodified BAC (#1), as the curing age extended, the compressive strength of BAC showed a gradually increasing trend, but the compressive strength at 14-day and 28-day was very low, almost unable to form strength, which clearly demonstrated the necessity of modifying the bamboo aggregate. Among the modified samples, those with a setting accelerator added generally exhibited higher compressive strengths at both 14-day and 28-day ages compared to those without a setting accelerator. This indicates that the preparation of BAC should consider the addition of a setting accelerator to promote cement hydration. Samples modified by different agents showed various performance. For silane coupling agent modification (#2), KH560 modification (#3), nano-penetration water-repellent modification (#4), sodium silicate solution modification (#5), sodium alginate-modified bamboo aggregate (#6), aluminum stearate modification (#7), and polyacrylate emulsion modification (#8), they all contributed to the improvement of compressive strength to different degrees compared to the unmodified sample. Among the seven modifiers, the concrete prepared with sodium alginate-modified bamboo aggregate (#6) showed the highest compressive strength, reaching 6.35 MPa at both 14-day and 28-day. In comparison, the compressive strength of Ordinary Concrete (OC) is significantly higher than that of BAC. Overall, bamboo-aggregate modification is crucial for enhancing BAC's compressive strength, with the addition of a setting accelerator and sodium alginate modification showing great promise, but further exploration and optimization are imperative for BAC to be more viable in construction-material applications.

3.2. Optimization of bamboo aggregate modification process

3.2.1. Determination of the range of influencing factors

Adding the accelerator $CaCl_2$ to BAC enhances the fluidity of freshly mixed concrete. During the experiments, it was observed that adding both a water-reducer and the accelerator to BAC caused bleeding in the freshly mixed concrete. As a result, in subsequent experiments, the water-reducer was omitted while the accelerator was retained, and the water consumption was reduced. The test mixture ratio was adjusted

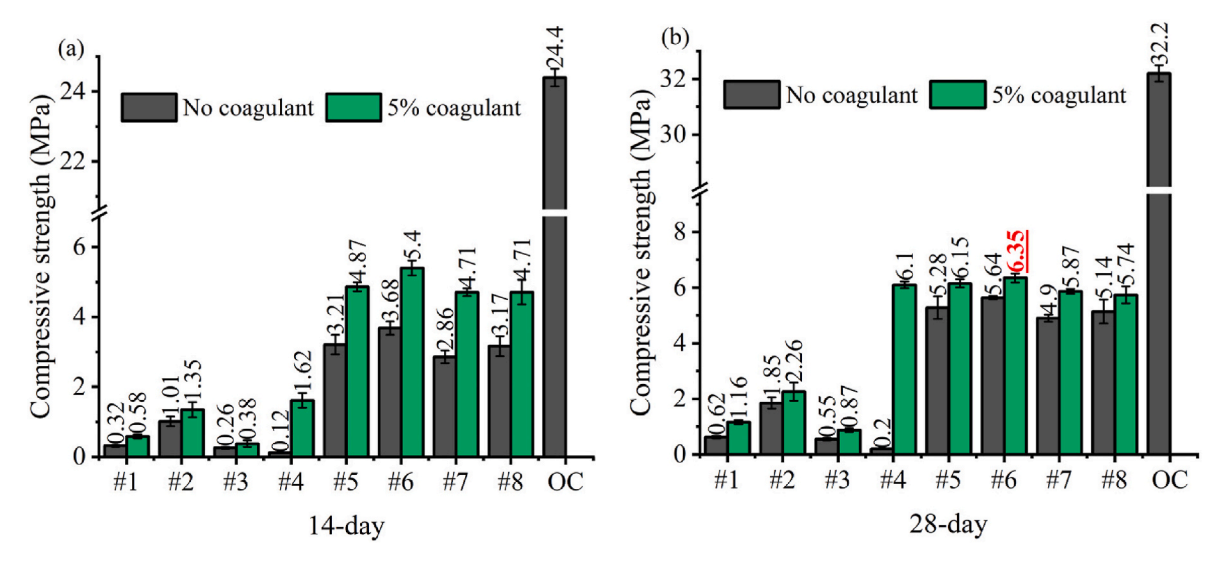


Fig. 4. Compressive strength of BAC with different modifications. (a) Curing age of 14-day; (b) Curing age of 28-day.

accordingly, and the adjusted mixture ratio is shown in Table 5.

Sodium alginate forms a viscous liquid when dissolved in water. It was found that in 60 $^{\circ}$ C warm water, when the concentration exceeds 0.5 %, sodium alginate does not dissolve well, causing flocculation. This leads to weak areas in the hardened BAC and a reduction in strength. Therefore, the concentration range of sodium alginate was set between 0.1 % and 0.5 %. The sodium in sodium alginate reacts with calcium to form a gel film, which improves the bonding strength between the bamboo aggregate and the cement matrix. Hence, a modified solution using CaCl₂ and sodium alginate was adopted. Based on the reaction principle, the Na-Ca ratio in the solution is 2:1, and the concentration range of the CaCl₂ solution is 0.1 %–0.3 %. Additionally, to address the issue of BAC not setting and hardening, the dosage range of the accelerator CaCl₂ was set between 10 % and 30 % (by weight of cement).

3.2.2. Results of the response surface experiment

With 68-day compressive strength as the response value and the concentration of sodium alginate, the concentration of $CaCl_2$, and the $CaCl_2$ coagulant dosage as independent variables, a response surface experiment was designed. The BAC was tested for compressive strength under the designed experimental conditions, and the experimental design and results are shown in Table 6.

In statistical analysis, the P-value represents the significance of the correlation coefficient. A P-value<0.0001 indicates extremely significant results, a P-value<0.01 is considered very significant, a P-value<0.05 is significant, and a P-value>0.05 is not significant. Table 7 presents a comprehensive analysis of various fitting models for different independent variables and their relationship with compressive strength. According to Table 7, the P-value for the linear model, the bifactor model, and the cubic polynomial fitting were not significant. However, the quadratic polynomial model had a P-value<0.0001, indicating extreme significance. Both its adjusted R^2 and predicted R^2 values were greater than 0.9, significantly higher than those of other models. Therefore, the quadratic polynomial prediction model was selected for this experiment. The response surface analysis method was used to analyze the data, resulting in the predictive model Equation (4).

Table 5The adjusted experimental mix proportion of BAC.

| Cement (kg/m ³) | Water (kg/m³) | Bamboo aggregates (kg/m³) | Sand (kg/m ³) | W/ C | Welan gum (%) |
|-----------------------------|------------------|---------------------------|------------------------------|---------|---------------------|
| 410.4 | 205.2 | 275 | 508.9 | 0.5 | 0.5 |

Table 6Response surface test results.

| Testing order | Indepen | dent varia | ble | Response value (Y) | SD | |
|---------------|--------------------|--------------------|--------------------|--------------------------------------|------|--|
| number | X ₁ (%) | X ₂ (%) | X ₃ (%) | 68-day age compressive strength(MPa) | • | |
| 1 | 0.3 | 0.2 | 20 | 7.9 | 0.32 | |
| 2 | 0.3 | 0.1 | 30 | 7.2 | 0.28 | |
| 3 | 0.5 | 0.2 | 10 | 6.2 | 0.42 | |
| 4 | 0.3 | 0.2 | 20 | 8.1 | 0.35 | |
| 5 | 0.5 | 0.2 | 30 | 6.0 | 0.45 | |
| 6 | 0.3 | 0.2 | 20 | 7.9 | 0.30 | |
| 7 | 0.1 | 0.2 | 30 | 7.6 | 0.29 | |
| 8 | 0.3 | 0.2 | 20 | 8.0 | 0.33 | |
| 9 | 0.3 | 0.3 | 30 | 6.8 | 0.40 | |
| 10 | 0.3 | 0.1 | 10 | 7.1 | 0.31 | |
| 11 | 0.3 | 0.2 | 20 | 7.7 | 0.27 | |
| 12 | 0.1 | 0.1 | 20 | 7.6 | 0.34 | |
| 13 | 0.1 | 0.2 | 10 | 6.9 | 0.37 | |
| 14 | 0.5 | 0.1 | 20 | 6.7 | 0.43 | |
| 15 | 0.3 | 0.3 | 10 | 6.6 | 0.41 | |
| 16 | 0.5 | 0.3 | 20 | 5.6 | 0.31 | |
| 17 | 0.1 | 0.3 | 20 | 7.4 | 0.36 | |

Table 7Model fit summary.

| Source | Sequential <i>P</i> -value | Lack of fit P-value | Adjusted R ² | Predicted R ² | Remarks |
|-----------|----------------------------|------------------------|----------------------------|-----------------------------|-----------|
| Linear | 0.0552 | 0.0036 | 0.2998 | 0.1546 | / |
| 2FI | 0.8290 | 0.0021 | 0.1635 | -0.2499 | / |
| Quadratic | < 0.0001 | 0.6079 | 0.9656 | 0.9030 | Suggested |
| Cubic | 0.6079 | | 0.9602 | | / |

$$Y = 2.46437 + 11.4625X_1 + 17.025X_2 + 0.26775X_3 - 11.25X_1X_2 -0.1125X_1X_3 + 0.025X_2X_3 - 16.8125X_1^2 - 42.25X_2^2 - 0.005725X_3^2$$
(4)

Table 8 shows the results of the analysis of variance for the predictive model, indicating that the model is extremely significant. Among the three factors, both X_1 and X_2 had P-value less than 0.01, reaching a very significant level, while X_3 had a P-value of 0.0793, which is greater than 0.05. This suggests that the concentration of sodium alginate and the concentration of CaCl $_2$ have a more substantial effect on the 68-day compressive strength, whereas the dosage of the coagulant CaCl $_2$ has a smaller impact. Considering the P-value, the estimated values from the system, and the degree of interaction, the influence of the three factors

Table 8Analysis of variance of prediction model.

| Source | Sum of squares | d_f | Mean square | F-value | P-value |
|-------------|----------------|-------|-------------|---------|----------|
| Model | 8.71 | 9 | 0.9673 | 50.91 | < 0.0001 |
| X_1 | 3.12 | 1 | 3.12 | 164.47 | < 0.0001 |
| X_2 | 0.6050 | 1 | 0.6050 | 31.84 | 0.0008 |
| X_3 | 0.0800 | 1 | 0.800 | 4.21 | 0.0793 |
| X_1X_2 | 0.2025 | 1 | 0.2025 | 10.66 | 0.0138 |
| X_1X_3 | 0.2025 | 1 | 0.2025 | 10.66 | 0.0138 |
| X_2X_3 | 0.0025 | 1 | 0.0025 | 0.1316 | 0.7275 |
| X_1^2 | 1.9 | 1 | 1.9 | 100.22 | < 0.0001 |
| X_2^2 | 0.7516 | 1 | 0.7516 | 39.56 | 0.0004 |
| X_3^2 | 1.38 | 1 | 1.38 | 72.63 | < 0.0001 |
| Residual | 0.1330 | 7 | 0.0190 | / | / |
| Lack of Fit | 0.0450 | 3 | 0.0150 | 68.18 | 0.6079 |
| Pure Error | 0.0880 | 4 | 0.0220 | / | / |
| Cor Total | 8.84 | 16 | / | / | / |

 $R^2 = 0.9850, R^2(Adj) = 0.9656.$

on the 68-day compressive strength, ranked from highest to lowest, is as follows: sodium alginate concentration, $CaCl_2$ concentration, and the dosage of coagulant $CaCl_2$. The interactions X_1X_2 , X_1X_3 , X_1^2 , X_2^2 , and X_3^2 are significant, with X_1X_2 , X_1X_3 , and X_2^2 having P-value<0.05, indicating significance, while X_1^2 and X_3^2 have P-value<0.0001, indicating extreme significance. The lack of fit term represents the degree of fit between the model and the experimental data; in this experiment, the lack of fit term of 0.6079 > 0.05, showing that the established model is reliable. The coefficient of determination, $R^2(Adj)=0.9656$, indicating that there is good consistency between the actual values and the predicted values of the 68-day compressive strength.

The response surface 3D plots and contour plots can visually reflect the degree of interaction effects on the response value. The steeper the surface and the denser the contour lines, which are closer to an ellipse shape, the stronger the interaction between two factors. Conversely, the closer the contour lines are to a circle, the weaker the interaction between the two factors. Fig. 5(a) display the influence of the interaction between sodium alginate concentration and CaCl2 concentration on the 68-day compressive strength when the dosage of the coagulant CaCl2 is 20 %. As the concentrations of sodium alginate and CaCl₂ increase, the compressive strength of BAC initially increases and then decreases. Moreover, the response surface for sodium alginate concentration is steeper than that for CaCl2 concentration, indicating that sodium alginate concentration has a greater impact on the compressive strength of BAC. The elliptical shape of the contour plot signifies that the interaction between the two factors significantly affects the 68-day compressive strength. Fig. 5(b) illustrate the effect of the interaction between sodium alginate concentration and the dosage of coagulant CaCl2 on the 68-day compressive strength when CaCl2 concentration is 0.2 %. Similar to the previous case, as the concentration of sodium alginate and the dosage of CaCl2 increase, the compressive strength of BAC follows a pattern of increasing and then decreasing. Additionally, the contour plot is elliptical, indicating a significant interaction effect on the 68-day compressive strength. Fig. 5(c) depict the influence of the interaction between CaCl2 concentration and the dosage of coagulant CaCl2 on the 68-day compressive strength when the sodium alginate concentration is 0.3 %. The response surface slope is relatively gentle, and the contour lines are close to circular, suggesting that the interaction between the two factors does not have a significant impact on the 68-day compressive strength of the concrete. The results of the response surface and contour line analysis are consistent with the analysis of variance.

Fig. 6(a) presents the normal probability plot of residuals from the experimental design results. The residuals are plotted on the horizontal axis, and the distribution probability is on the vertical axis. The points in the plot generally lie close to a straight line, indicating that the fitted model has good accuracy within the given range. Fig. 6(b) shows the predicted vs. actual plot, with the horizontal axis representing the experimental values and the vertical axis representing the predicted

values from the model. The distribution of points near the line also suggests that the predictive model is in good agreement with the actual situation.

3.2.3. Validation of the response surface predictive model

To verify the validity of the predictive model based on the response surface methodology, the predicted values of the model were compared with the actual experimental values. According to the predictive model, when the concentration of sodium alginate is 0.2 %, the concentration of CaCl2 is 0.18 %, and the dosage of the coagulant CaCl2 is 21.73 %, the compressive strength of BAC reaches its maximum value, with a predicted value of 8.10 MPa. When the sodium alginate concentration is 0.48 %, the calcium chloride concentration is 0.30 %, and the coagulant dosage is 12.44 %, the compressive strength of BAC reaches its minimum value, with a predicted value of 5.57 MPa. By controlling the concentrations of sodium alginate and CaCl₂ and the coagulant CaCl₂ dosage, compressive tests were carried out on BAC. The test results are shown in Table 9. The actual measured values obtained according to the model's predicted maximum value were 7.64 MPa, 7.81 MPa, and 7.93 MPa, with corresponding errors of 6.0 %, 3.7 %, and 2.1 %, respectively, and all errors between the measured and predicted values were less than 10 %. Similarly, the actual measured values obtained according to the model's predicted minimum value were 5.67 MPa, 5.72 MPa, and 5.78 MPa, with corresponding errors of approximately 1.8 %, 2.6 %, and 3.6 %, respectively, and again, all errors between the measured and predicted values were less than 10 %. Therefore, the effectiveness of the response surface predictive model was confirmed through experimental verification.

3.3. SEM test results and analysis

Observing the microstructure of the bamboo aggregate using a SEM enables a more intuitive understanding of the synergistic modification principle of sodium alginate-CaCl2. From Fig. 7(a), the protruding burrs on the surface of the bamboo aggregate are clearly visible, which are a result of the sample cutting process. These burrs are detrimental to the strength formation of BAC material, as they can easily form weak interfaces. Observing Fig. 7(b) and (c), after treatment with the sodium alginate process, the surface of the bamboo aggregate appears cleaner and clearer, and it is evident that the sodium alginate gel has filled the fine cracks on the surface of the bamboo aggregate, making it denser. From the microscopic surface, a continuous network structure can be observed. This network structure is formed by the ionic exchange reaction between Ca²⁺ from CaCl₂ and Na⁺ from sodium alginate, which results in the formation of a cross-linked calcium alginate gel. This crosslinked network structure acts as a "molecular adhesive," filling the micro-pores and cracks on the bamboo aggregate surface. The reduction of surface defects significantly decreases stress concentration sites during loading, enhancing the aggregate's resistance to crack propagation. The calcium alginate gel also improves the wettability between the hydrophilic bamboo fibers and the cementitious matrix. According to the interfacial energy theory, a lower interfacial tension facilitates better mechanical interlocking. The gel layer not only provides a physical barrier but also forms hydrogen bonds with the hydrated products of cement (e.g., C-S-H gel), forming a better interface transition zone. This molecular-level adhesion effectively transfers stress from the mortar to the aggregate, preventing premature debonding. Furthermore, the crosslinked network structure exhibits viscoelastic properties. Under compressive loading, the calcium alginate gel can dissipate energy through molecular chain deformation, acting as a buffer against sudden stress surges. This energy dissipation mechanism, combined with the enhanced stiffness provided by the filled voids, collectively contributes to the improved load-bearing capacity of BAC.

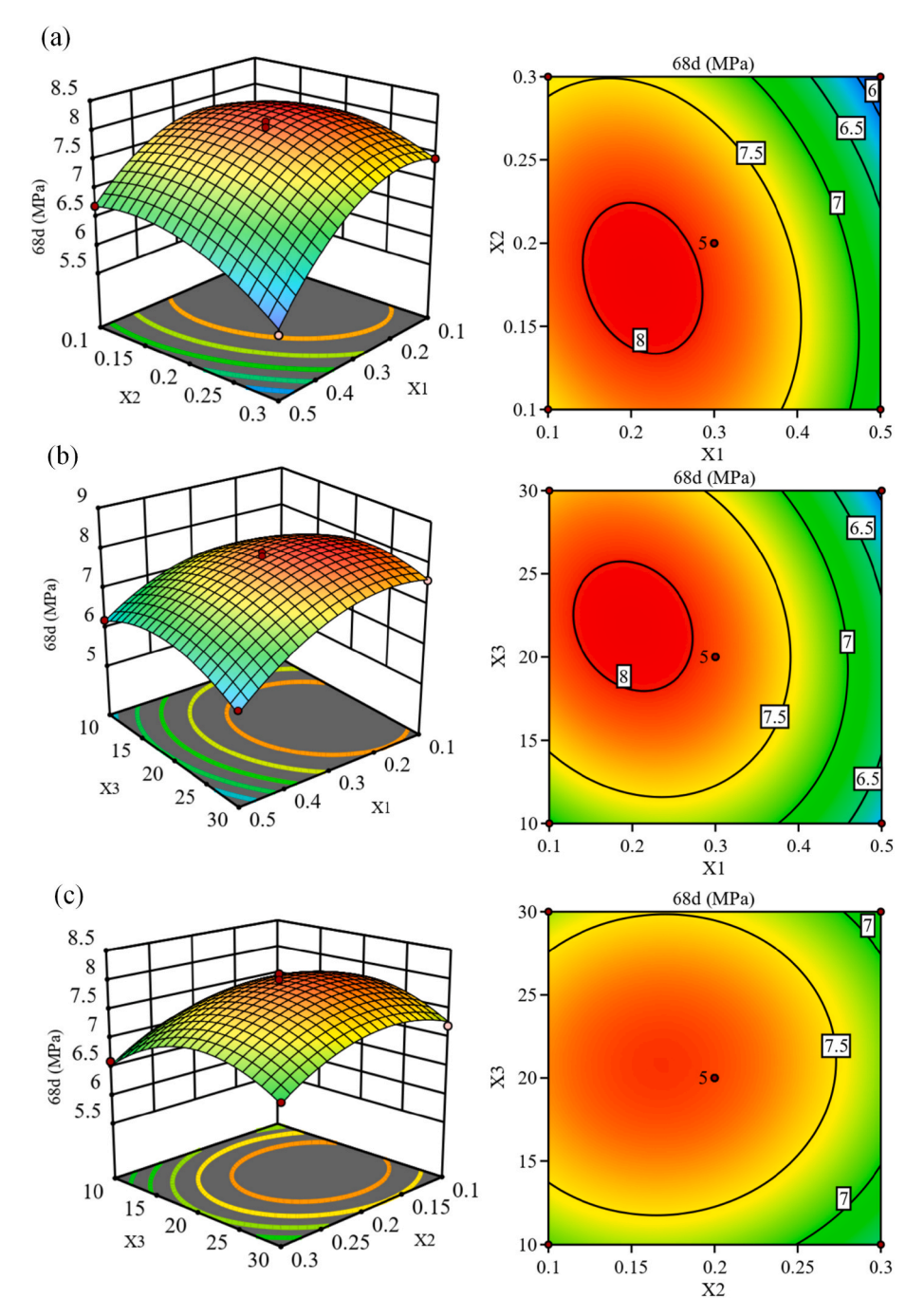


Fig. 5. Response surface and contour plots of interactions. (a) represent the interaction between X_1 and X_2 ; (b) represent the interaction between X_1 and X_3 ; (c) represent the interaction between X_2 and X_3 .

3.4. Physical and mechanical property tests of BAC specimens

3.4.1. The effect of bamboo aggregate grading on concrete performance

Considering the distinctive properties of bamboo aggregate as a biomass-lightweight aggregate, researching the performance of BAC with different gradations is of great significance. According to the previously-mentioned sodium alginate modification process parameters and concrete mix design, cubic specimens were prepared for testing their 28-day compressive strength, dry apparent density, and water absorption rate. Fig. 8 illustrates the impact of bamboo aggregate gradation on the compressive strength of concrete. G0 represents 0 % of 5–10 mm and 100 % of 10–15 mm bamboo aggregates; G30 represents 30 % of 5–10 mm and 70 % of 10–15 mm, and others follow the same rule. As the proportion of bamboo aggregate with a particle size of 5 mm–10 mm

increases, the compressive strength first decreases and then increases. It reaches a peak value of 8.73 MPa when the concrete cube is made up entirely of 5 mm–10 mm bamboo aggregate. Notably, the strength of G30 is the lowest. This is because the bamboo aggregate, crushed by a blade crusher, has a flat, rectangular shape, which makes it difficult to mix uniformly. When a small amount of fine bamboo aggregate is added, it cannot fill the gaps between the larger aggregates evenly and tends to accumulate in one place, thereby reducing the compressive strength of the concrete. However, as the content of fine bamboo aggregate gradually increases, it can be well-mixed to form a uniform and dense structure, leading to a gradual increase in the compressive strength of the concrete.

Fig. 9 shows the effect of bamboo aggregate gradation on the dry apparent density of concrete. In contrast, as the content of fine bamboo

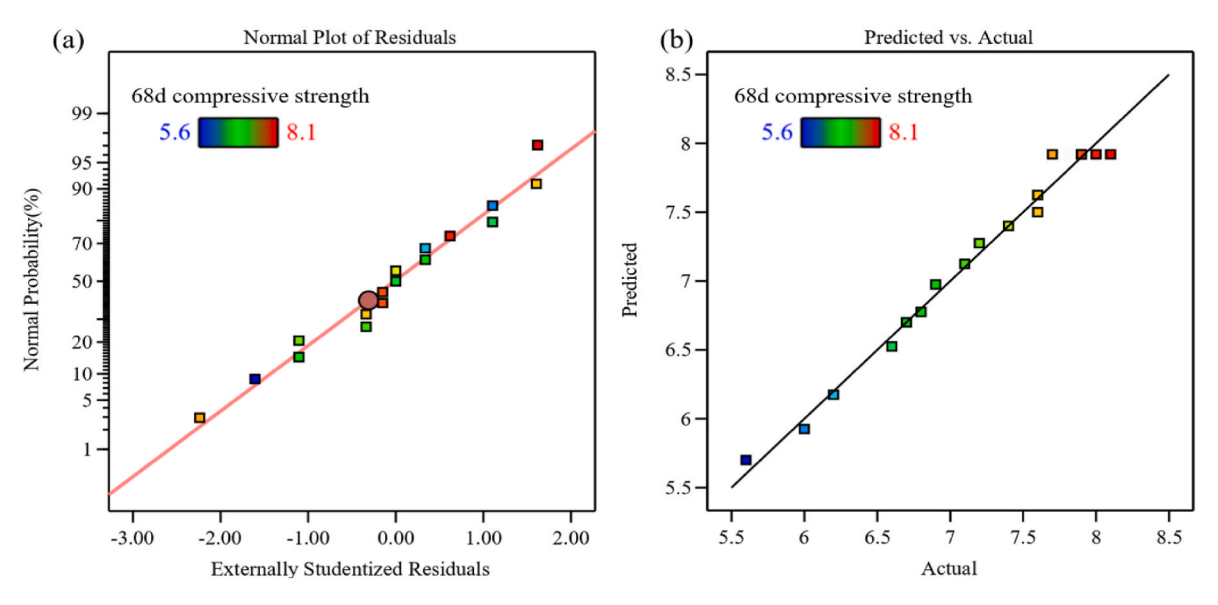


Fig. 6. Regression model analysis. (a) Normal probability plot of residuals; (b) Predicted vs actual.

Table 9Comparison of predicted and experimental values.

| Name | Predicted value(MPa) | Experimental value(MPa) | SD (MPa) | Error (%) |
|--|-------------------------|-------------------------|----------------------|-------------------|
| Predicted maximum compressive strength | 8.10 | 7.64 7.81 7.93 | 0.31 0.28 0.35 | 6.0 3.7 2.1 |
| Predicted minimum compressive strength | 5.57 | 5.67 5.72 5.78 | 0.31 0.23 0.33 | 1.8 2.6 3.6 |

aggregate increases, the dry apparent density of the concrete shows a downward trend. Specifically, when the bamboo aggregate particle size is entirely in the 10~mm-15~mm range, the dry apparent density is $1340~\text{kg/m}^3$, and when it is entirely in the 5~mm-10~mm range, the dry apparent density is $1280~\text{kg/m}^3$, representing a decrease of 4.48~%. This is due to the fact that the density of the part of the bamboo closer to the 'bamboo green' is greater than that of the 'bamboo yellow', and its hardness is also higher. During the crushing process, the 'bamboo green' part mainly forms larger-sized bamboo aggregate, while the 'bamboo yellow' part mainly forms finer-sized aggregate. Therefore, BAC with a particle size of 10~mm-15~mm has the highest dry apparent density.

Fig. 10 depicts the influence of bamboo aggregate gradation on the water absorption of concrete. Similarly, it is found that as the content of fine bamboo aggregate increases, the water absorption rate of the

concrete also rises. The reason is that a higher content of fine bamboo aggregate increases the total specific surface area of the aggregate, resulting in a higher water absorption rate. In conclusion, to obtain BAC material with lighter weight and higher strength, it is advisable to use bamboo aggregate with a particle size of 5 mm–10 mm.

This study further realizes reasonable control over the particle shape of bamboo aggregate. As stipulated in "Lightweight Aggregates and Their Test Methods-Part 2" (GB/T 17431.2-2010), the shape coefficient is a technical indicator used to describe the geometric characteristics of lightweight aggregates. It is defined as the ratio of the longest dimension to the smallest dimension of the middle cross-section of the aggregate particles. Bamboo aggregate is obtained by crushing and sieving Moso bamboo. Due to the hollow structure of bamboo and the operation of the crushing equipment, bamboo aggregate mainly takes on a flat form. When using the shape coefficient for description, it can only control the shape dimensions in the length and width directions and fails to represent its thickness dimension. Therefore, it is inappropriate to use the shape coefficient to objectively characterize the particle shape of bamboo aggregate. This paper proposes a more suitable method and parameter for describing the morphology of bamboo aggregate. The basic idea is that as a coarse aggregate, bamboo aggregate itself needs to have better mechanical properties, meaning the flatness of the bamboo aggregate should be smaller and the thickness greater. A new technical indicator is proposed to reflect the thickness of the bamboo aggregate, namely the Bamboo Aggregate Mass Index (BAMI), to describe the particle shape of bamboo aggregate. A higher BAMI value indicates that

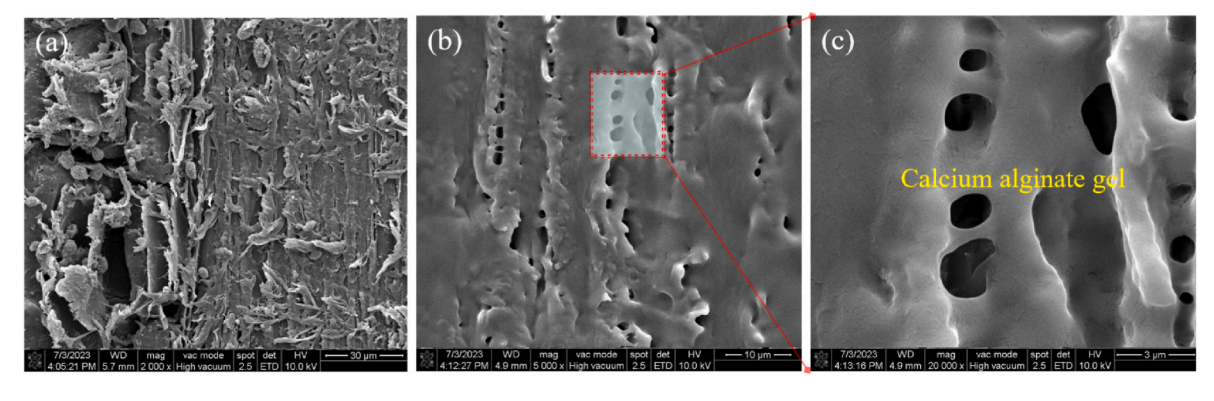


Fig. 7. Microscopic morphology of the bamboo aggregate. (a) represent the unmodified bamboo aggregate; (b) and (c) represent the sodium alginate-modified bamboo aggregate.

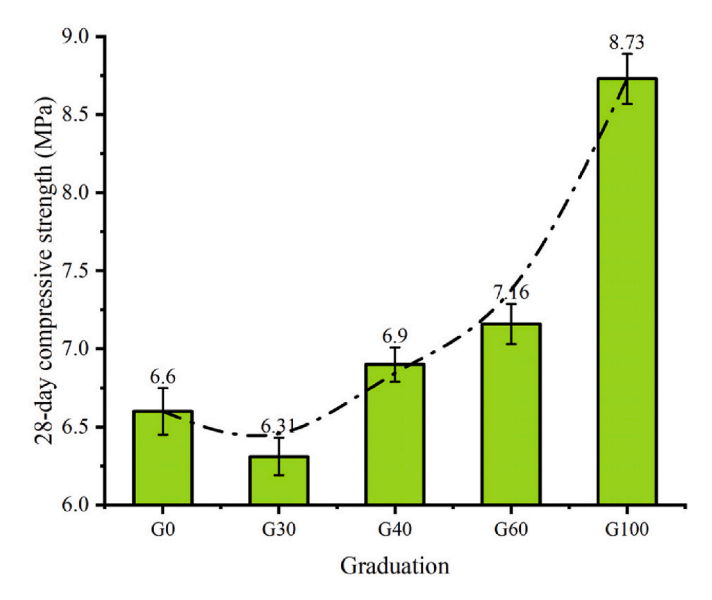


Fig. 8. Influence of bamboo aggregate gradation on the compressive strength of concrete.

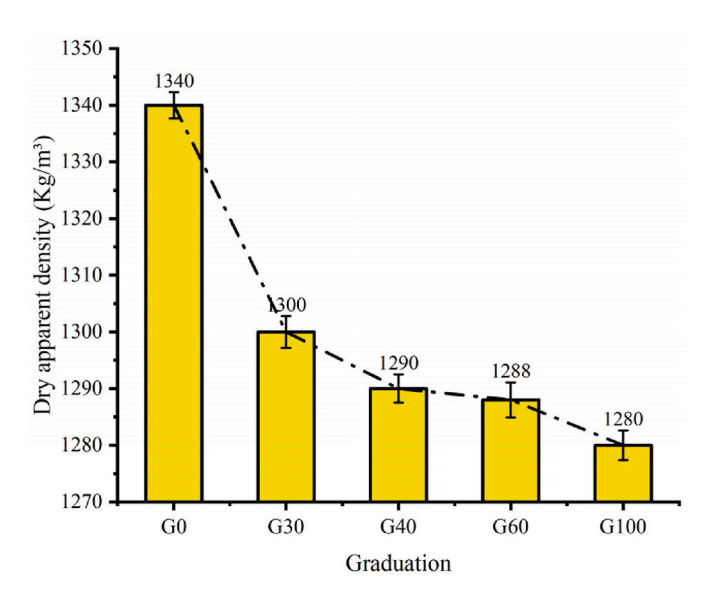


Fig. 9. The influence of bamboo aggregate gradation on the dry apparent density of concrete.

bamboo aggregates of the same length and width are thicker, thus having better mechanical properties. Randomly selected groups A, B, C, D, and E of bamboo aggregates with a particle size of 5-10 mm were tested, with 50 particles in each group. BAMI is calculated according to formula (5). Fig. 11(a) shows the distribution of BAMI values for randomly tested groups of bamboo aggregates with a particle size of 5-10 mm. The test results show that over 82.4 % of the bamboo aggregates have a BAMI value greater than 0.4. The thickness of the bamboo aggregates was statistically analyzed in ascending order, and the distribution pattern of bamboo aggregate thickness is shown in Fig. 11(b). It can be seen from the figure that the maximum thickness corresponding to a BAMI value less than 0.4 is 2.1 mm. The smaller the thickness of the bamboo aggregate, the worse its mechanical strength. The preparation quality of bamboo aggregate can be improved by optimizing the crushing level of bamboo aggregate, and then based on the BAMI value, particle shape control and evaluation can be conducted.

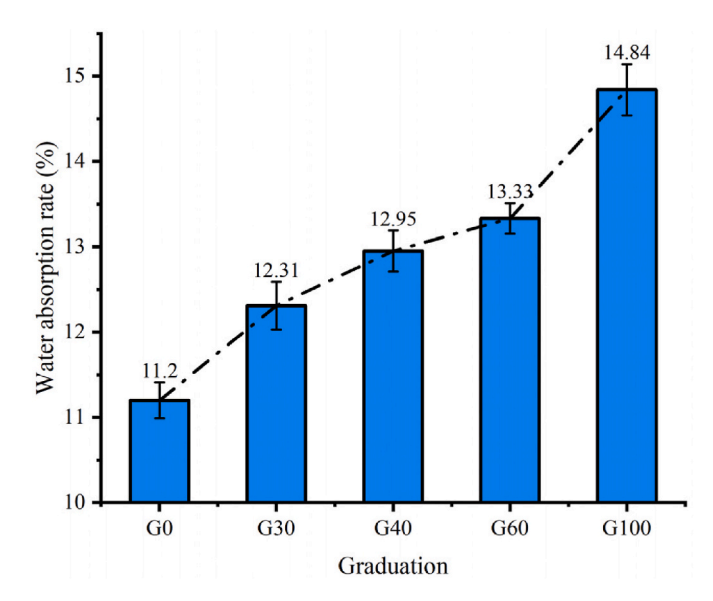


Fig. 10. Influence of bamboo aggregate gradation on the water absorption of concrete.

$$BAMI = \frac{M^*1000}{L^2}$$
 (5)

In the equation: M represents the mass of the bamboo aggregate, in grams (g); L represents the length of the long side of the bamboo aggregate, in millimeters (mm).

3.4.2. The influence of fly ash content on concrete performance

Bamboo aggregate is susceptible to degradation in the alkaline environment of the mortar matrix. Fly ash can react with the hydration product, calcium hydroxide (Ca(OH)₂), to form low-alkalinity calcium silicate hydrate (C-S-H) gels. This reaction reduces the alkalinity of the mortar matrix, which has a positive impact on the durability of bamboo aggregate. In the experiments, the fly-ash content varied from 0 % to 30 % by the weight of cement, and the related test results are presented as follows. As depicted in Fig. 12, the 28-day compressive strength of BAC shows a clear downward trend as the fly-ash content increases. When there is no fly ash (0 % fly-ash content), the 28-day compressive strength of BAC is 6.9 MPa. As the fly-ash content reaches 30 %, the 28-day compressive strength drops to 4.72 MPa, representing a significant reduction of 31.59 %. This decrease is mainly due to the lower reactivity of fly ash compared to cement. Fly ash has a slower hydration rate, which delays the overall hydration reaction of the concrete and thus reduces the early-stage compressive strength. For the 180-day compressive strength, although it also decreases with the increase of fly-ash content, the reduction is less pronounced than that of the 28-day strength. At 0 % fly-ash content, the 180-day compressive strength is 7.2 MPa, and at 30 % fly-ash content, it is 6.7 MPa. This indicates that over a longer period, the negative impact of fly-ash addition on compressive strength is mitigated to some extent, likely because the secondary hydration reaction of fly ash gradually contributes to the strength

Fig. 13 illustrates the relationship between fly-ash content and the dry apparent density of BAC. Both the 28-day and 180-day dry apparent densities increase as the fly-ash content rises. Starting from 1290 kg/m³ at 0 % fly-ash content for the 28-day dry apparent density, it reaches 1360 kg/m³ at 30 % fly-ash content, which is an increase of 5.43 %. The 180-day dry apparent density shows a similar pattern, increasing from 1295 kg/m³ at 0 % fly-ash content to 1358 kg/m³ at 30 % fly-ash content. This increase in density can be attributed to the physical filling effect of fly-ash particles in the concrete matrix. Fly-ash particles, with their fine-grained nature, fill the voids between larger cement particles

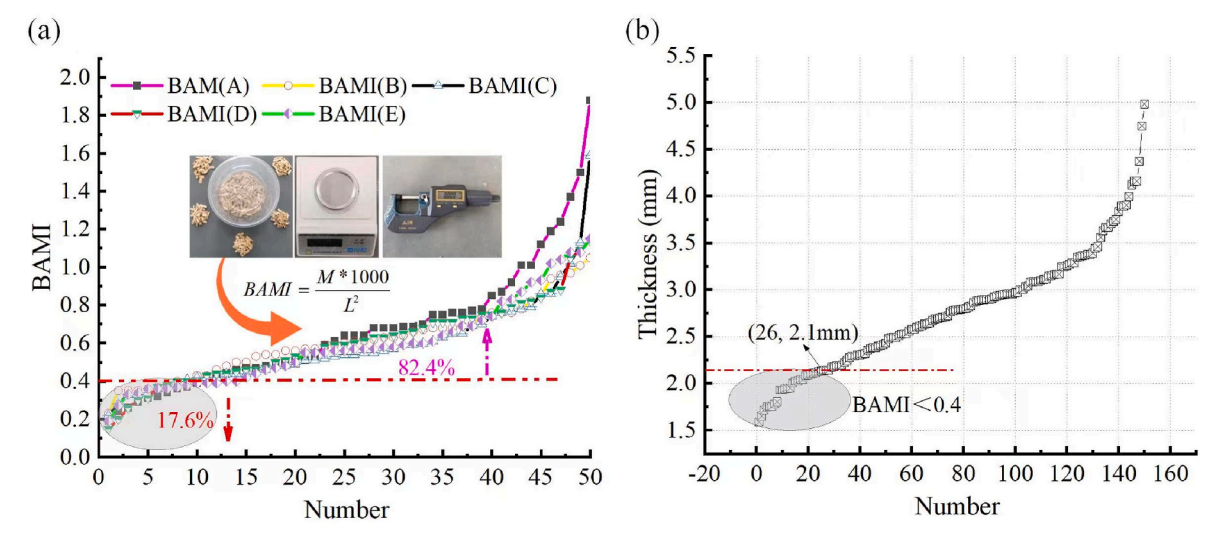
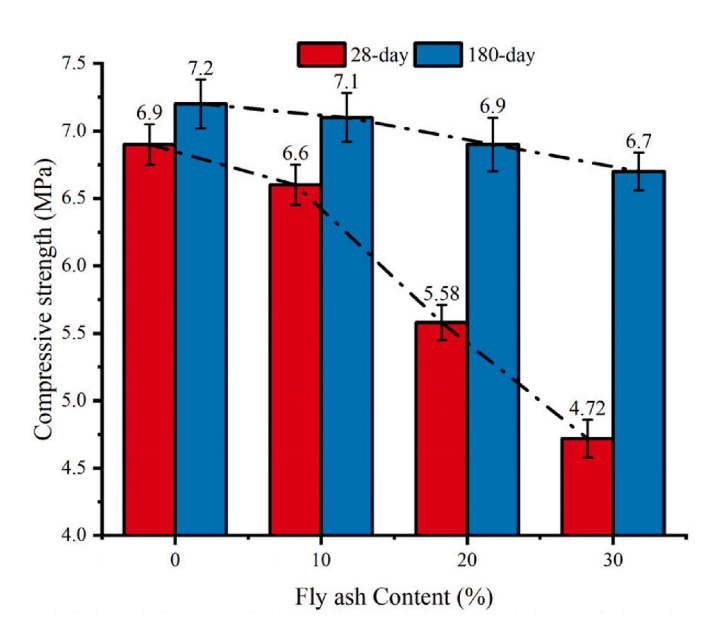


Fig. 11. (a)BAMI distribution; (b)Distribution of bamboo aggregate thickness.



 $\textbf{Fig. 12.} \ \ \textbf{Influence of fly ash content on the compressive strength of concrete.}$

and aggregates, resulting in a more compact structure and thus an increase in density. However, the 5.43~% increase is relatively small, suggesting that the impact of fly-ash addition on density is not extremely significant.

Fig. 14 reveals that an increase in fly-ash content leads to a gradual rise in the water absorption rate of the concrete. For the 28-day water absorption rate, compared to the concrete without fly ash (13.33 % at 0 % fly-ash content), the concrete with 30 % fly-ash content has a water absorption rate of 17.46 %, representing a considerable increase of 30.98 %. The 180-day water absorption rate also shows an upward trend, increasing from 12.89 % at 0 % fly-ash content to 17.01 % at 30 % fly-ash content. The reason for this increase is that as the fly-ash content increases, the hydration process is slowed down. Before the fly-ash and cement particles are fully hydrated, more pores and voids exist in the concrete matrix, which allows more water to be absorbed. In conclusion, in the short term, fly ash does not have a positive effect on the properties of BAC. The reduction in compressive strength, relatively small increase in density, and significant rise in water absorption rate are all unfavorable factors. However, due to the secondary hydration reaction of fly ash and its low-alkalinity characteristic, over the long term, the

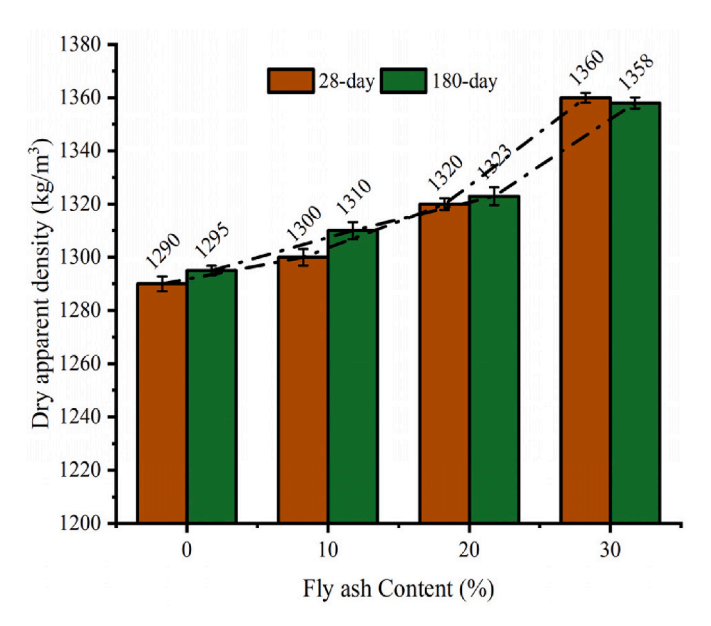


Fig. 13. The influence of fly ash content on the dry apparent density of concrete.

continuous progress of hydration has the potential to enhance the long-term durability of BAC materials.

3.5. Discussion

The optimized sodium alginate modification method for bamboo aggregates shows great promise in practical applications. For pedestrian walkway pavements, as required by the "Green Building Evaluation Standard", using bamboo aggregates with a particle size of 5–10 mm offers a remarkable alternative to traditional concrete materials. In comparison with traditional aggregates, bamboo aggregates are more lightweight, yet they can still provide sufficient strength for pedestrianlevel loads.

Moreover, the insights into the role of fly ash in BAC performance have valuable implications for concrete mixture design. Although fly ash has been found to cause a reduction in short-term compressive strength, its long-term benefits in enhancing durability cannot be overlooked. By carefully adjusting the mix design and ensuring proper curing conditions, the positive effects of fly ash can be maximized. The response

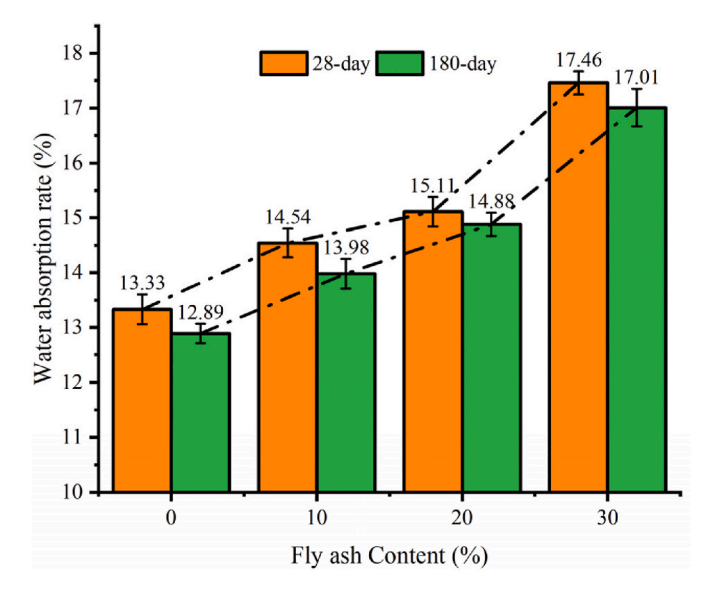


Fig. 14. Influence of fly ash content on the water absorption of concrete.

surface methodology-optimized process parameters also play a crucial role. In industrial production, these parameters can serve as a reliable reference. They ensure that the BAC produced has consistent quality and performance. This consistency is vital for large-scale manufacturing, as it allows for better quality control and reduces the variability in product characteristics. It also enables more efficient production processes, as manufacturers can rely on these optimized parameters to streamline their operations.

Despite these positive aspects, the study has several limitations that point to the need for further research. The long-term durability of BAC, particularly in harsh environmental conditions such as freeze-thaw cycles and high-humidity environments, remains a major area of concern. Additionally, the long-term stability of the sodium alginate gel, which is crucial for the bonding performance in BAC, has not been fully explored. Continuous monitoring and in-depth evaluation of these aspects are essential. For instance, long-term exposure tests in real-world harsh environments, such as coastal areas with high salt content or regions with extreme temperature variations, can provide more accurate data on the durability of BAC. Another significant limitation is the lack of comprehensive economic and environmental analysis. A life-cycle assessment of BAC production, which includes aspects such as raw material extraction, manufacturing processes, transportation, and endof-life disposal, was not carried out in this study. Understanding the economic viability and environmental impact of BAC throughout its entire life cycle is essential for its widespread adoption. Future research should focus on this aspect, comparing BAC with traditional construction materials in terms of cost-effectiveness, energy consumption, and carbon footprint. This will provide a more complete picture of the feasibility and sustainability of BAC as a construction material, enabling more informed decision-making in the construction industry.

4. Conclusion

This study developed BAC by substituting traditional crushed stone with bamboo aggregate and using sodium alginate for modification. Among seven methods, the sodium alginate-CaCl₂ synergistic was most effective, yielding a 28-day compressive strength of 8.10 MPa. Response surface methodology optimized the parameters: 0.20 % sodium alginate concentration, 0.18 % CaCl₂ concentration, and 21.73 % CaCl₂ accelerator dosage. SEM analysis showed that sodium alginate gel filled bamboo aggregate micro-cracks, forming a cross-linked network to strengthen interfacial bonding with mortar. A key innovation is the BAMI, which accurately evaluates bamboo aggregate particle shape.

Higher BAMI values indicate better mechanical properties. Using 5–10 mm bamboo aggregate with a high BAMI reduced BAC dry apparent density to $1280~{\rm kg/m^3}$ and achieved 8.73 MPa compressive strength, balancing lightness and strength. Although fly ash reduces 28-day strength, its low alkalinity and secondary hydration benefit long-term durability. The optimized BAC can serve as an option for pedestrian pavements. In the future, comprehensive economic and environmental analyses should be carried out, with a focus on the long-term durability monitoring and evaluation of BAC in harsh environments.

CRediT authorship contribution statement

Xiang Chen: Writing – original draft, Supervision, Software, Investigation, Formal analysis, Data curation. Hongzhou Zhu: Writing – review & editing, Supervision, Resources, Funding acquisition. Xinqiang Zhang: Writing – review & editing, Visualization, Validation, Supervision, Resources, Funding acquisition. Dan Yang: Software, Project administration, Investigation, Formal analysis. Zhenzhen Wang: Writing – original draft, Project administration, Investigation. Jian Zhang: Project administration, Investigation, Data curation. Jian Zhang: Writing – review & editing, Visualization, Validation, Resources, Methodology.

Disclosure statement

No potential conflict of interest was reported by the author(s).

Declaration of competing interest

The authors declare that they have no known competing financial interests or personal relationships that could have appeared to influence the work reported in this paper.

Acknowledgements

The authors would like to acknowledge the financial support for this study provided by the Chongqing Natural Science Foundation Innovation and development joint fund project, China (CSTB2022NSCQ-LZX0063) and the Joint Training Base Construction Project for Graduate Students in Chongqing (JDLHPYJD2020014) and the Project supported by Building Environment Engineering Technology Research Center in Dazhou (Sichuan University of Arts and Sciences), Dazhou 635000, China (SDJ2024ZB-09).

Data availability

Data will be made available on request.

References

Ban, Y., Zhi, W., Fei, M.E., Liu, W.D., Yu, D.M., Fu, T.F., Qiu, R.H., 2020. Preparation and performance of cement mortar reinforced by modified bamboo fibers. Polymers 12 (11), 2650.

Birniwa, A.H., Abdullahi, S.S., Ali, M., Mohammad, R.E.A., Jagaba, A.H., Amran, M., Avudaiappan, S., Maureira-Carsalade, N., Flores, E.I.S., 2023. Recent trends in treatment and fabrication of plant-based fiber-reinforced epoxy composite: a review. J. Composites Sci. 7 (3), 120.

Blandino, A., Macias, M., Cantero, D., 1999. Formation of calcium alginate gel capsules: influence of sodium alginate and CaCl2 concentration on gelation kinetics. J. Biosci. Bioeng. 88 (6), 686–689.

Chen, J., Su, X., Zheng, M., Lin, J., Tan, K.B., 2022. Enhanced properties of chitosan/ hydroxypropyl methylcellulose/polyvinyl alcohol green bacteriostatic film composited with bamboo fiber and silane-modified bamboo fiber. Polym. Compos. 43 (4). 2440–2449.

Chen, X., Zhu, H.Z., Yang, X.Y., Huang, C.X., 2024. Development of anti-segregation device and uniformity evaluation for all-bamboo aggregate concrete. Constr. Build. Mater. 425, 135974.

Chin, S.C., Tee, K.F., Tong, F.S., Doh, S.I., Gimbun, J., 2020. External strengthening of reinforced concrete beam with opening by bamboo fiber reinforced composites. Mater. Struct. 53 (6), 1–12.

- Escamilla, E.Z., Habert, G., 2014. Environmental impacts of bamboo-based construction materials representing global production diversity. J. Clean. Prod. 69, 117–127.
- Huang, P., Latif, E., Chang, W.-S., Ansell, M.P., Lawrence, M., 2017. Water vapour diffusion resistance factor of Phyllostachys edulis (Moso bamboo). Constr. Build. Mater. 141, 216–221.
- Idris, N.a., Noh, H.M., Zor, M.F.M., Wahab, N.S.A., 2021. A review on the used of bamboo as aggregate in concrete with different type of treatment. Multidiscipl. Appl. Res. Innovat. 2 (2), 70–78.
- Kang, J.T., Park, S.H., Kim, S.H., 2014. Improvement in the adhesion of bamboo fiber reinforced polylactide composites. J. Compos. Mater. 48 (21), 2567–2577.
- Li, J., Hou, Q.M., Zhang, X.Q., Zhang, X.B., 2025. Microbial-induced mineral carbonation: a promising approach for improving Carbon sequestration and performance of steel slag for its engineering utilization. Dev. Built Environ. 21, 100615.
- Li, Z.Z., Luan, Y., Hu, J.B., Fang, C.H., Liu, L.T., Ma, Y.F., Liu, Y., Fei, B.H., 2022. Bamboo heat treatments and their effects on bamboo properties. Constr. Build. Mater. 331, 127320
- Lima, H.C., Willrich, F.L., Barbosa, N.P., Rosa, M.A., Cunha, B.S., 2008. Durability analysis of bamboo as concrete reinforcement. Mater. Struct. 41 (5), 981–989.
- Liu, D.G., Song, J.W., Anderson, D.P., Chang, P.R., Hua, Y., 2012. Bamboo fiber and its reinforced composites: structure and properties. Cellulose 19 (5), 1449–1480.
- Liu, W.D., Qiu, R.H., Li, K.C., 2016. Effects of fiber extraction, morphology, and surface modification on the mechanical properties and water absorption of bamboo fibersunsaturated polyester composites. Polym. Compos. 37 (5), 1612–1619.
- Manimaran, A., Somasundaram, M., Ravichandran, P., 2017. Experimental study on partial replacement of coarse aggregate by bamboo and fine aggregate by quarry dust in concrete. Int. J. Civ. Eng. Technol. 8 (8), 1019–1027.
- Mohan, N., Dash, S.P., Boby, N.M., Shetty, D., 2022. Study of bamboo as a building material–Construction & preservation techniques and its sustainability. Mater. Today Proc. 60, 100–114.
- Mudjanarko, S.W., Limantara, A.D., Mayestino, M., Sutrisno, A.E.A., Ibrahim, M.H.W., Wiwoho, F.P., 2020. The utilization of bamboo innovation as aggregate substitute for paving block. In: Journal of Physics: Conference Series. IOP Publishing, 012014.

- Sari, F.F., Limantara, A.D., Ridwan, A., Gardjito, E., Subiyanto, B., Sudarmanto, H.L., Widayati, S.C., Windradi, F., Setiono, G.C., Rahman, I., Mudjanarko, S.W., Iop, 2020. Laboratory testing on the standard mixed designed paving with bamboo material as smooth and rough aggregate. In: 5th International Conference on Civil and Environmental Engineering for Sustainability (IConCEES), 012032. Senai, MALAYSIA.
- Tahara, R., Hasnan, M., Azizan, N., 2021. Performance of beting bamboo (Gigantochloa Levis) as partial replacement for coarse aggregate in concrete. In: IOP Conference Series: Earth and Environmental Science. IOP Publishing, 012014.
- van der Lugt, P., van den Dobbelsteen, A., Janssen, J.J.A., 2006. An environmental, economic and practical assessment of bamboo as a building material for supporting structures. Constr. Build. Mater. 20 (9), 648–656.
- Wang, G.F., Wei, Y., Wang, J.Q., Zhou, Z.Y., Chen, S.B., Zhu, B.R., 2024a. Assessment of the properties of interface-modified bamboo aggregates for sustainable concrete construction. J. Build. Eng. 94, 110069.
- Wang, G.F., Wei, Y., Zhu, B.R., Wang, J.Q., Chen, S., Huang, S.L., 2024b. Stress-strain relationship of biomass concrete with bamboo as coarse aggregates under uniaxial compression. J. Mater. Res. Technol. 32, 1011–1027.
- Wang, Q.Y., Han, H., Lou, Z.C., Han, X., Wang, X., Li, Y.J., 2022. Surface property enhancement of bamboo by inorganic materials coating with extended functional applications. Compos. Appl. Sci. Manuf. 155, 106848.
- Yu, D.W., Tan, H.W., Ruan, Y.J., 2011. A future bamboo-structure residential building prototype in China: life cycle assessment of energy use and carbon emission. Energy Build. 43 (10), 2638–2646.
- Yuan, T.C., Yin, X.S., Huang, Y.Q., Li, X.R., Wang, X.Z., Chen, L., Li, Y.J., 2022. Hydrothermal treatment of bamboo and its effect on nano-mechanic and antimildew property. J. Clean. Prod. 380, 135189.
- Zactiti, E.M., Kieckbusch, T.G., 2009. Release of potassium sorbate from active films of sodium alginate crosslinked with calcium chloride. Packag. Technol. Sci. 22 (6), 340, 358
- Zhou, Z.Y., Wei, Y., Wang, G.F., Wang, J.Q., Lin, Y., Zhu, B.R., 2024. Experimental study on the basic properties of new biomass bamboo aggregate concrete. J. Build. Eng. 86, 108892.